Mathematical Modelling of Confidence Ellipses and Computational Validation of their Implementation in the LFTools Plugin: A Case Study Using GWDBrazil

Leandro França[1], Tiago Silvano[2], Savia Gavazza[3], Simone Sato[4]

[1] Dept. of Civil Engineering, Federal University of Pernambuco (UFPE), Recife, Brazil – leandro.silvafranca@ufpe.br
[2] Dept. of Cartographic Engineering, Federal University of Pernambuco (UFPE), Recife, Brazil – tiago.prudencio@ufpe.br
[3] Dept. of Civil Engineering, Federal University of Pernambuco (UFPE), Recife, Brazil – savia@ufpe.br
[4] Dept. of Cartographic Engineering, Federal University of Pernambuco (UFPE), Recife, Brazil – simone.sato@ufpe.br

Keywords: Confidence Ellipse, Spatial Statistics, Covariance Matrix, QGIS, GWDBrazil.

Abstract

Confidence ellipses are widely used in spatial analysis to summarize the central tendency, dispersion and directional structure of bivariate point distributions. Although conceptually grounded in the covariance matrix and the properties of the bivariate normal distribution, their computational implementation in GIS environments requires rigorous validation to ensure statistical consistency and reproducibility. This study presents the mathematical formulation, algorithmic design and empirical evaluation of the *Confidence Ellipses* tool implemented in the LFTools plugin for QGIS. The method is based on covariance–variance estimation, eigenvalue decomposition and Chi-square scaling, enabling the generation of ellipses corresponding to confidence levels of 68%, 90%, 95% and 99%. A controlled validation using 100,000 Gaussian random points confirmed the numerical accuracy of the tool, with observed proportions of points inside the ellipses deviating less than 0.05% from theoretical expectations. A real-world application using 351,256 groundwater wells from the Groundwater Well Database for Brazil (GWDBrazil) demonstrated the tool’s capacity to represent complex spatial patterns, including anisotropy, clustering and non-Gaussian behavior. The results indicate that the LFTools implementation is mathematically sound, computationally robust and suitable for scientific use in spatial statistics and environmental analysis. Future research may extend this framework to multiscale, non-parametric and space–time formulations, enabling deeper characterization of spatial phenomena across regions, whether in Brazil or throughout the world.

1. Introduction

Confidence ellipses, also referred to as concentration, error, variance, or directional ellipses, remain among the most established and versatile statistical summaries for bivariate spatial point distributions, providing a compact representation of central tendency, dispersion, and directional structure (Erten and Deutsch, 2020; Friendly et al., 2013; Gong, 2002). Originally introduced by Lefever (1926) to quantify geographic concentration, the method has been widely adopted and refined in GIS and spatial statistics, where it is particularly useful for describing anisotropy and directional trends in real-world spatial phenomena (Reyna-Sevilla et al., 2023; Wang et al., 2015). In practical terms, a confidence ellipse summarizes not only where a set of events is concentrated, but also how it spreads and aligns directionally, properties that are central to interpreting spatial patterning in applied geospatial analysis.

From a statistical standpoint, confidence ellipses follow directly from the bivariate normal model: iso-density contours are ellipses, and ellipse sizes associated with common confidence levels (e.g., 68%, 90%, 95%, and 99%) are obtained via Chi-square scaling with two degrees of freedom, yielding probabilistic coverage regions when Gaussian assumptions are approximately met (Erten and Deutsch, 2020; Friendly et al., 2013; Jobson, 2012; Wang et al., 2015). The ellipse orientation is determined by the eigenvectors of the variance–covariance matrix, which define the principal axes of the distribution; the semi-axis lengths depend on the eigenvalues, enabling the ellipse geometry to express directional variability and anisotropy (Friendly et al., 2013; Jobson, 2012; Mardia et al., 1979). Figure 1 illustrates typical isotropic and directional cases, highlighting how differences in variances and the presence of covariance yield circular or elongated ellipses with a well-defined major axis.

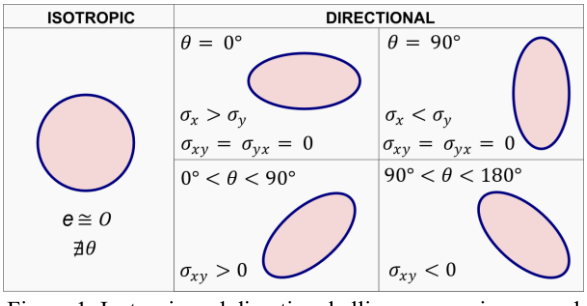

Figure 1. Isotropic and directional ellipses on variances and covariances.

1.1 Related work / state of the art

Confidence/standard deviational ellipses continue to be used across several applied domains because they provide an interpretable summary of complex spatial patterns. In

This contribution has been peer-reviewed. The double-blind peer-review was conducted on the basis of the full paper.
https://doi.org/10.5194/isprs-annals-XI-4-2026-171-2026

geosciences, ellipses have been employed to characterize directional clustering and spatial organization in mineral-related point patterns and deposit clusters (Mamuse et al., 2009). In public health and spatial accessibility studies, ellipse-based representations are used to describe activity spaces and spatial footprints relevant to service accessibility and disease-related mobility patterns (Sherman et al., 2005), while spatiotemporal analyses of infectious disease events also benefit from compact summaries of dispersion and directional tendencies (Dong et al., 2017). In crime geography, deviational ellipses have supported the identification of structured crime patterns and have been applied in criminal geographic profiling workflows (Kent and Leitner, 2007). In meteorology and engineering-oriented analyses, ellipses have been used to summarize directional properties of trajectories and event distributions (Rahman et al., 2018), and to represent spatial uncertainty in lightning-location estimates through assigned confidence ellipses (Diendorfer et al., 2014). Ellipse-based summaries have also been adopted in urban/industrial contexts for describing spatiotemporal distributions and shifting gravity centres (Ayhan and Cubukcu, 2010; Song et al., 2017), as well as in assessments of the quality of volunteered geographic information (Forghani and Delavar, 2014). At the same time, the literature documents that misuse or overinterpretation of confidence ellipses can lead to misleading conclusions, reinforcing the need for transparent implementations and careful methodological reporting (Rocchi et al., 2005).

1.2 Motivation and contribution

With the expansion of remote sensing, large-scale geocoding, and high-density geospatial databases, there is increasing demand for methods that are both mathematically rigorous and computationally reproducible, particularly in open-source environments (Gahegan, 2023; Koldasbayeva et al., 2024). In QGIS (QGIS Development Team, 2025), algorithmic transparency is essential for scientific auditability and reliable reuse. Although centrographic summaries such as confidence/standard deviational ellipses remain widely applied in spatial investigations (Hu et al., 2025), few studies explicitly validate whether a GIS implementation reproduces the expected probabilistic coverage under controlled conditions. This gap is particularly relevant in open-source GIS environments, where methodological transparency and reproducibility are essential for scientific reliability. Therefore, beyond presenting the mathematical modelling underpinning confidence ellipses (covariance structure, eigen-decomposition, and Chi-square scaling), this work performs an empirical validation of the Confidence Ellipses tool implemented in the LFTools plugin for QGIS. The validation follows a coverage-by-counting procedure across multiple confidence levels using simulated bivariate Gaussian data, and is complemented by a real-world case study using the Groundwater Well Database for Brazil (GWDBrazil), a harmonized repository with over 350,000 groundwater wells (Uchôa et al., 2025a; Uchôa et al., 2025b). This combined strategy ensures that the implementation is not only faithful to the formal model, but also robust when applied to large, non-Gaussian spatial datasets.

2. Mathematical Formulation of the Confidence Ellipse

2.1 General Ellipse Representation

Using matrix algebra notation, a confidence ellipse associated with a set of points $P_i(x_i, y_i)$ can be expressed by Equation (1):

$$[x-\overline{x}\;\; y-\overline{y}]\Sigma^{-1}\begin{bmatrix}x-\overline{x}\\ y-\overline{y}\end{bmatrix}=S, \tag{1}$$

Where $\bar{x}$ and $\bar{y}$ are the means of the x and y coordinates, defining the center of the ellipse; Σ is the variance–covariance matrix; and S is a positive scalar that determines the size of the ellipse according to the desired confidence level.

The variance–covariance matrix Σ is given by Equation (2):

$$\Sigma=\begin{bmatrix}\sigma_x^2 & \sigma_{xy}\\ \sigma_{yx} & \sigma_y^2\end{bmatrix}, \tag{2}$$

where σ_x^2 and σ_y^2 are the variances of x and y, and $\sigma_{xy}=\sigma_{yx}$ corresponds to the covariance between these variables.

The value of the scalar S may be chosen arbitrarily (for example, $S=1$). However, when the goal is to represent a confidence interval, such as 68%, 90%, 95%, or 99%, one must rely on the Chi-Square distribution. This is because, in the bivariate case, the sum of the squares of two independent, normally distributed variables follows a Chi-Square distribution with two degrees of freedom (Friendly et al., 2013; Jobson, 2012). Thus, for each confidence level there is a specific value of S, obtained from the inverse cumulative distribution function of this distribution.

Table 1 presents the values of S computed using the stats.chi2.ppf command from the Python SciPy library.

Probability (%)	39,35	68	90	95	99
S	1	2.2789	4.6052	5.9915	9.2103

Table 1. S values for different confidence levels.

In cases where the covariance is null ($\sigma_{xy}=\sigma_{yx}=0$), Equation (1) reduces to:

$$[XY]\begin{bmatrix}1/\sigma_x^2 & 0\\ 0 & 1/\sigma_y^2\end{bmatrix}\begin{bmatrix}X\\ Y\end{bmatrix}=S, \tag{3}$$

where $X=x-\bar{x}$ and $Y=y-\bar{y}$.

By expanding the matrix product, one obtains the classical form of the ellipse equation:

$$\frac{X^2}{\sigma_x^2}+\frac{Y^2}{\sigma_y^2}=S\;\therefore\;\frac{X^2}{S\sigma_x^2}+\frac{Y^2}{S\sigma_y^2}=1\;\therefore\;\frac{x^2}{a^2}+\frac{y^2}{b^2}=1, \tag{4}$$

where the semi-axes are given by:

$$a=\sqrt{S}\sigma_x,\qquad b=\sqrt{S}\sigma_y.$$

2.2 Ellipse Orientation Based on Eigenvalues and Eigenvectors

When the covariance is non-zero, the resulting ellipse is no longer aligned with the Cartesian axes, requiring the determination of its orientation in the plane. To this end, the classical approach consists of computing the eigenvectors and eigenvalues of the matrix associated with the quadratic form of the ellipse, allowing it to be diagonalized and eliminating the mixed XY term (Friendly et al., 2013; Jobson, 2012).

The eigenvectors v_1 and v_2, associated with the eigenvalues λ_1 and λ_2, define an orthogonal basis that enables the construction of the rotation matrix P (Equation 5), which transforms the original coordinate system (X, Y) into a new system (X', Y') aligned with the principal axes of the ellipse. In this basis, the diagonal matrix D (Equation 6) contains the eigenvalues along its diagonal, representing the directions of maximum and minimum variability.

$$P = \begin{bmatrix} v_{1_x} & v_{2_x} \\ v_{1_y} & v_{2_y} \end{bmatrix}, \tag{5}$$

$$D = P^T A P = \begin{bmatrix} \lambda_1 & 0 \\ 0 & \lambda_2 \end{bmatrix}, \tag{6}$$

Since $PP^T = I$, we obtain $A = \Sigma^{-1} = PDP^T$ and, by applying the coordinate transformation $[X'Y'] = [XY]P$, the general equation of the ellipse can be rewritten in diagonal form (Equation 7), free of the correlation term. In this orthogonal system, the ellipse has axes aligned with the eigenvectors and its semi-axes are given by as illustrated in Figure 2.

$$[X \;\; Y] P D P^T \begin{bmatrix} X \\ Y \end{bmatrix} = S \quad \therefore$$

$$[X' \;\; Y'] D \begin{bmatrix} X' \\ Y' \end{bmatrix} = S \quad \therefore$$

$$[X' \;\; Y'] \begin{bmatrix} \lambda_1 & 0 \\ 0 & \lambda_2 \end{bmatrix} \begin{bmatrix} X' \\ Y' \end{bmatrix} = S \tag{7}$$

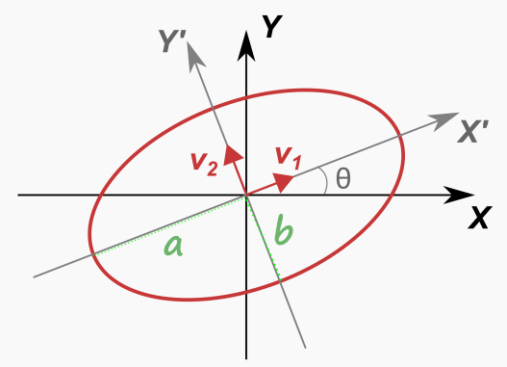

Figure 2. Rotated ellipse aligned with the principal axes of variability.

3. Computational Implementation in LFTools

LFTools is an open-source plugin developed for QGIS, designed to automate cartographic, topographic, and spatial statistics workflows. The plugin is available both in the official QGIS Plugin Manager and in a public GitHub repository, ensuring code transparency, the possibility of independent auditing, and full reproducibility of results across different working environments.

Among the modules in the **“Spatial Statistics”** group of LFTools, the **“Confidence Ellipses”** tool stands out, developed to generate ellipses based on the variance–covariance matrix of a set of points. In practical terms, the algorithm receives a point layer as input, such as the groundwater well layer from GWD-Brazil, and allows the user to select the desired confidence level (68%, 90%, 95%, or 99%), as well as optionally define weighting and grouping fields (Figure 3). As output, the tool produces a polygon layer containing one or more standard deviational ellipses, each summarizing the mean location, spatial dispersion, and directional orientation of the corresponding point set.

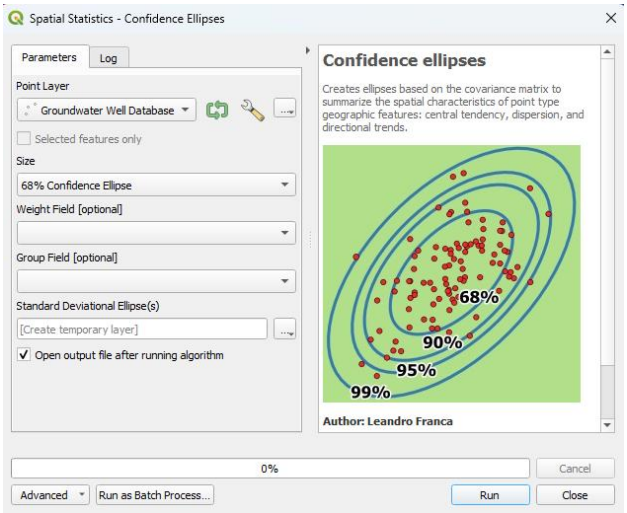

Figure 3. Interface of the Confidence Ellipses tool from the LFTools plugin in QGIS.

From a computational standpoint, the tool’s code directly implements the matrix-based modeling discussed in the theoretical section. For each group of points (or for the full dataset, when no grouping field is provided), the algorithm extracts the x and y coordinates and, when available, their respective weights. Following this, it:

- computes the weighted mean of the coordinates $(\bar{x}, \bar{y})$, which defines the center of the ellipse;
- obtains the variance–covariance matrix using the numpy.cov function, with or without weights;
- performs eigenvalue–eigenvector decomposition (numpy.linalg.eig), from which it identifies the axis of maximum variability (the eigenvector associated with

This contribution has been peer-reviewed. The double-blind peer-review was conducted on the basis of the full paper.
https://doi.org/10.5194/isprs-annals-XI-4-2026-171-2026 | © Author(s) 2026. CC BY 4.0 License.

the largest eigenvalue) and computes the semi-axis lengths;

- applies the scaling factor $\sqrt{S}$, where S is the fixed value corresponding to the selected confidence level (2.27887, 4.60517, 5.99146, 9.21034), derived from the Chi-Square distribution with two degrees of freedom (Table 1);
- constructs the ellipse vertices by trigonometric parameterization, rotates them according to the angle ϕ obtained from the principal eigenvector, and finally translates the figure to the center $(\bar{x}, \bar{y})$.

Each generated feature is enriched with descriptive attributes, including mean X and Y coordinates, standard deviations along both axes, the selected confidence level, the rotation angle (in degrees), and the lengths of the major and minor axes, thereby enabling precise quantitative interpretation and deeper analytical insight within a GIS environment.

In this way, the **Confidence Ellipses** tool explicitly and transparently implements the link between the theory of the bivariate normal distribution, the variance–covariance matrix, and the geometric representation of directional dispersion, ensuring full auditability and reproducibility of the method.

4. Validation of the Tool and Case Study

4.1 Statistical Validation Using Simulated Bivariate Gaussian Data

The validation stage aimed to assess whether the confidence ellipses produced by the Confidence Ellipses algorithm contain, to a close approximation, the proportions theoretically expected under a bivariate normal distribution, i.e., whether the empirical coverage associated with the 68%, 90%, 95%, and 99% confidence levels is reproduced under controlled simulation conditions.

The point dataset was generated externally in Python, following the same statistical model assumed by the method: independent Gaussian components along the principal axes, followed by a planar rotation. Specifically, n = 100,000 points were sampled with mean $(X_0, Y_0) = (0,0)$, standard deviations $\sigma_x = 200$ m and $\sigma_y = 100$ m, and rotation angle $\phi = 45°$, using numpy.random.normal and a 2D rotation matrix to obtain the final coordinates. The simulation was performed in a projected CRS (EPSG:5880 – SIRGAS 2000 / Brazil Polyconic) to ensure metric consistency for dispersion measures and ellipse geometry. These parameters match those available in the LFTools interface and are documented in the Python script used in this study. The parameters used in the simulation are illustrated in Figure 4.

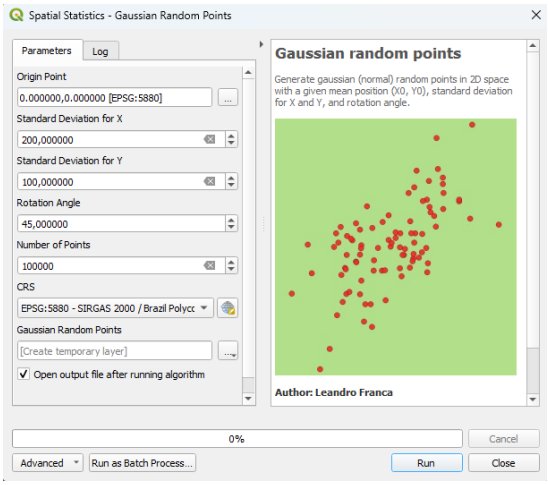

Figure 4. Parameters used to generate the simulated bivariate Gaussian point dataset.

The simulated point set was then processed with the Confidence Ellipses tool, producing ellipses for the four confidence levels. Empirical coverage was computed by counting the number of points contained within each ellipse polygon, enabling a direct comparison between observed proportions and the theoretical confidence levels implied by the Chi-square distribution with two degrees of freedom. Figure 5 illustrates the simulated point cloud and the resulting confidence ellipses.

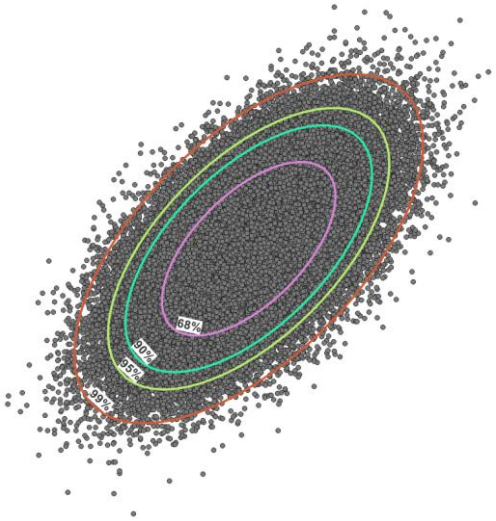

Figure 5. Simulated Gaussian points and the corresponding confidence ellipses.

The results of the point counts contained within each ellipse are summarized in Table 2.

Ellipse	Meaning	Points Inside	Percentage
68%	moderate confidence	67,995	67.995%
90%	high confidence	89,959	89.959%
95%	scientific standard	94,965	94.965%
99%	very high confidence	98,968	98.968%

Table 2. Point counts inside the confidence ellipses for the simulated Gaussian dataset.

The results show strong agreement with theoretical expectations, with errors below 0.05% across all confidence levels, thereby validating the numerical correctness of the

LFTools implementation. As expected for a bivariate normal model, the observed proportions closely match the reference values defined by the Chi-square quantiles for two degrees of freedom. This confirms that the tool is statistically consistent and reliable for applications requiring reproducible confidence ellipse estimation.

4.2 Empirical Application to Groundwater Wells in Brazil

To evaluate the tool under real-world conditions, we used the groundwater well dataset from the *Groundwater Well Database for Brazil* (GWDBrazil), which contains 351,256 records distributed across all Brazilian states (Figure 6).

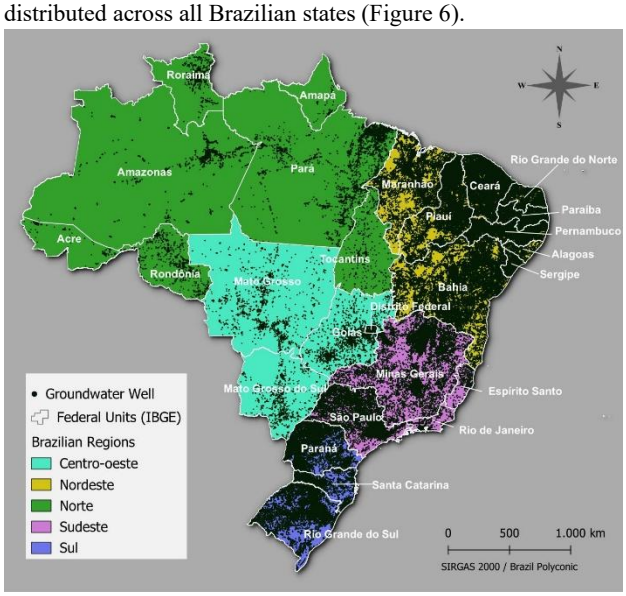

Figure 6. Wells from the GWDBrazil.

Based on this dataset, 68% confidence ellipses were generated for three different spatial extents:

1. The entire Brazilian territory
2. Major geographic regions of Brazil (Norte, Nordeste, Centro-Oeste, Sudeste, and Sul)

Figure 7 shows the 68% confidence ellipse for the full GWDBrazil dataset.

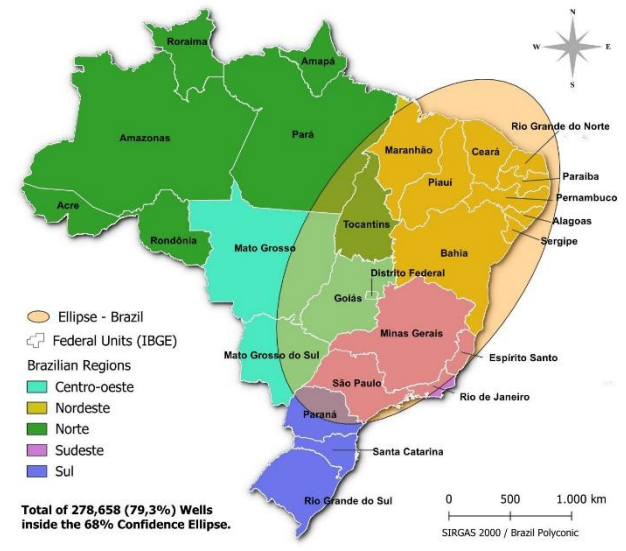

Figure 7. 68% confidence ellipse for the entire dataset.

The number of points within the 68% confidence ellipse for the national set of wells (Figure 7) resulted in 79.3% of the 351,256 records falling inside the generated ellipse. This value, higher than the theoretical interval expected for a bivariate normal distribution, does not arise from any inconsistency in the tool, but rather from inherent characteristics of the actual spatial distribution of GWDBrazil. The national pattern is marked by strong heterogeneity, with notable concentrations of wells in the Nordeste region, the presence of multiple hydrogeological clusters, as well as clear directional trends and structural anisotropies related to geology, hydrology, and human occupation of the territory. These factors, widely discussed in the literature (Wang, 2015), cause the empirical behaviour to deviate from bivariate normality, producing percentages above or below the theoretical value in practical applications.

For the regional analysis of Brazil, Figure 8 and Table 3 present the map of the confidence ellipses and the number of points within the generated ellipses.

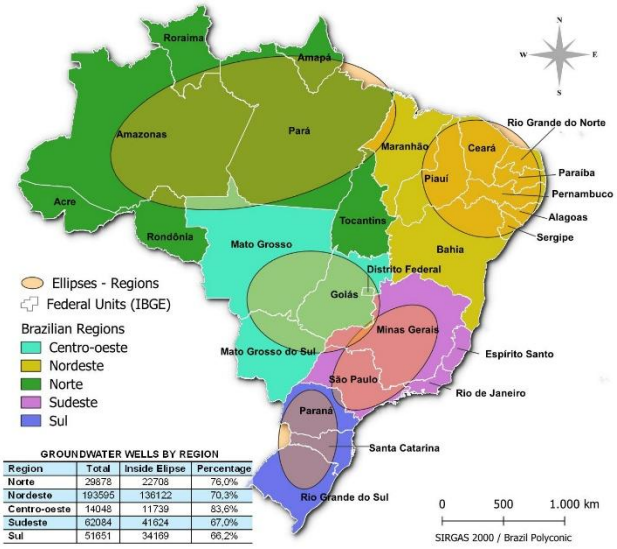

Figure 8. 68% confidence ellipses by region.

Region	Total	Inside Ellipse	Percentage
Norte	29878	22708	76,0%
Nordeste	193595	136122	70,3%
Centro-oeste	14048	11739	83,6%
Sudeste	62084	41624	67,0%
Sul	51651	34169	66,2%

Table 3. Groundwater wells by region and percentage contained within the ellipses

The regional analysis (Figure 8 and Table 3) reinforces this behavior and highlights important differences among the Brazilian macro-regions. The Centro-oeste showed the highest percentage of points contained within the ellipse (83.6%), indicating a more compact and homogeneous spatial distribution, consistent with the predominance of extensive aquifers, lower urban density, and greater continuity of hydrogeological formations. The Norte, with 76.0%, also

This contribution has been peer-reviewed. The double-blind peer-review was conducted on the basis of the full paper.
https://doi.org/10.5194/isprs-annals-XI-4-2026-171-2026 | © Author(s) 2026. CC BY 4.0 License.

exhibited strong relative concentration, although with marked anisotropy, since the wells tend to align with major hydrographic axes and settlement fronts along the deforestation arc. In contrast, the Nordeste, despite having the largest absolute number of wells, showed 70.3% within the ellipse, revealing a combination of large clusters in semiarid areas and dispersions associated with regional geological variations. The Sudeste (67.0%) and Sul (66.2%) regions had the lowest percentages, which is compatible with more fragmented distributions influenced by high urbanization, geological diversity, and the multiplicity of hydrographic basins, factors that increase dispersion and reduce adherence to the Gaussian model. Taken together, the results of Figures 7 and 8 confirm two central conclusions of the study: (i) the LFTools tool operates in a mathematically consistent manner, as demonstrated by validation with simulated Gaussian data; and (ii) in real applications, exact adherence to theoretical percentages is not expected, since the spatial structure of geographic phenomena tends to exhibit anisotropies, clusters, and non-Gaussian patterns, characteristics that the method faithfully captures by synthesizing the form, orientation, and dispersion actually present in the data.

5. Conclusion

This study presented a comprehensive investigation of mathematical modeling, computational implementation, and empirical validation of confidence ellipses applied to bivariate spatial distributions, with emphasis on the Confidence Ellipses tool of the LFTools plugin for QGIS. The formalization based on the variance–covariance matrix, spectral decomposition by eigenvalues and eigenvectors, and the rigorous use of the Chi-Square distribution proved sufficient to accurately describe the size, shape, and orientation of the ellipses, ensuring coherence between statistical foundations and their algorithmic translation. Experiments with 100,000 Gaussian points confirmed the fidelity of the implementation, showing that the observed percentages of 68%, 90%, 95%, and 99% adhere almost exactly to the theoretical values, with deviations below 0.05%. In the case study with the 351,256 GWDBrazil wells, the tool demonstrated the same robustness in synthesizing real spatial patterns marked by anisotropy, regional clusters, and strong non-normality, adequately reproducing the underlying spatial structures without relying on idealized distributional assumptions.

Overall, the results confirm that the LFTools implementation is mathematically sound, computationally stable, and fully suitable for scientific applications, aligned with contemporary guidelines of transparency, auditability, and reproducibility in GIS. The ellipses generated correctly capture directional trends and structural patterns across multiple scales, reinforcing the value of the tool for geographic, environmental, and hydrogeological analyses.

As future developments, it is recommended to deepen the investigation of the spatial distribution of wells at more detailed levels, states and municipalities, by incorporating spatiotemporal models, non-parametric methods for complex distributions, and clustering and multiscale analysis techniques. Such extensions can significantly expand the analytical capacity of confidence ellipses, enabling even more refined interpretations in environmental, urban, and territorial management applications.

The open-source availability of the implementation further supports independent verification and reproducible spatial analysis workflows.

References

Ayhan, I., Cubukcu, K. M., 2010. Explaining historical urban development using the locations of mosques: A GIS/spatial statistics-based approach. Applied Geography 30, 229–238. https://doi.org/10.1016/j.apgeog.2009.05.002.

Diendorfer, G., Pichler, H., Schulz, W., 2014. Euclid located strokes to the gaisberg tower–accuracy of location and its assigned confidence ellipse, in: Proceedings, International Lightning Detection Conference (ILDC), Tucson, United-States.

Dong, W., Yang, K., Xu, Q., Liu, L., Chen, J., 2017. Spatio-temporal pattern analysis for evaluation of the spread of human infections with avian influenza A(H7N9) virus in China, 2013–2014. BMC Infectious Diseases 17, 704. https://doi.org/10.1186/s12879-017-2781-2.

Erten, O., Deutsch, C.V., 2020. Combination of multivariate Gaussian distributions through error ellipses. Geostatistics Lessons. University of Alberta. https://geostatisticslessons.com.

Forghani, M., Delavar, M., 2014. A Quality Study of the OpenStreetMap Dataset for Tehran. ISPRS International Journal of Geo-Information 3, 750–763. https://doi.org/10.3390/ijgi3020750.

Friendly, M., Monette, G., Fox, J., 2013. Elliptical insights: understanding statistical methods through elliptical geometry. Statistical Science 28. https://doi.org/10.1214/12-STS402.

Gahegan, M., 2023. From Reproducible to Explainable GIScience (Short Paper). LIPIcs, Volume 277, GIScience 2023 277, 32:1-32:6. https://doi.org/10.4230/LIPICS.GISCIENCE.2023.32.

Gong, J., 2002. Clarifying the standard deviational ellipse. Geographical Analysis 34, 155–167. https://doi.org/10.1111/j.1538-4632.2002.tb01082.x.

Hu, H., Shao, H., Li, Y., Guan, M., Tong, J., 2025. GIS-based analysis of elderly care facility distribution and supply–demand coordination in the Yangtze river delta. Land 14, 723. https://doi.org/10.3390/land14040723.

Jobson, J.D., 2012. Applied multivariate data analysis: volume II: Categorical and Multivariate Methods. Springer Science & Business Media.

Kent, J., Leitner, M., 2007. Efficacy of standard deviational ellipses in the application of criminal geographic profiling. Journal of Investigative Psychology and Offender Profiling 4, 147–165. https://doi.org/10.1002/jip.72.

Koldasbayeva, D., Tregubova, P., Gasanov, M., Zaytsev, A., Petrovskaia, A., Burnaev, E., 2024. Challenges in data-driven geospatial modeling for environmental research and practice. Nature Communications 15, 10700. https://doi.org/10.1038/s41467-024-55240-8.

Lefever, D.W., 1926. Measuring geographic concentration by means of the standard deviational ellipse. American Journal of Sociology 32, 88–94.

Mamuse, A., Porwal, A., Kreuzer, O., Beresford, S., 2009. A new method for spatial centrographic analysis of mineral deposit clusters. Ore Geology Reviews 36, 293–305. https://doi.org/10.1016/j.oregeorev.2009.06.001.

Mardia, K.V., Kent, J.T., Bibby, J.M., 1979. Multivariate analysis. Academic Press, London.

QGIS Development Team, 2025. QGIS Geographic Information System. Open Source Geospatial Foundation Project. https://qgis.org.

Rahman, M., Yang, R., Di, L., 2018. Clustering Indian Ocean Tropical Cyclone Tracks by the Standard Deviational Ellipse. Climate 6, 39. https://doi.org/10.3390/cli6020039.

Reyna-Sevilla, A., Gonzalez-Castañeda, M., Ramos-Herrera, I., Duque-Molina, C., Borrayo-Sanchez, G., Aviles-Hernandez, R., Quezada-Sanchez, C., Flores-Morales, A., 2023. A geospatial model to identify areas associated with late-stage breast cancer: A spatial epidemiology approach. Asian Pacific Journal of Cancer Prevention 24, 2621–2628. https://doi.org/10.31557/APJCP.2023.24.8.2621.

Rocchi, M.B.L., Sisti, D., Ditroilo, M., Calavalle, A., Panebianco, R., 2005. The misuse of the confidence ellipse in evaluating statokinesigram. Italian Journal of Sport Science 12, 169–172.

Sherman, J.E., Spencer, J., Preisser, J.S., Gesler, W.M., Arcury, T.A., 2005. A suite of methods for representing activity space in a healthcare accessibility study. International Journal of Health Geographics 4, 24. https://doi.org/10.1186/1476-072X-4-24.

Song, Y., Gui, Z., Wu, H., Wei, Y., 2017. A WEB-BASED FRAMEWORK FOR VISUALIZING INDUSTRIAL SPATIOTEMPORAL DISTRIBUTION USING STANDARD DEVIATIONAL ELLIPSE AND SHIFTING ROUTES OF GRAVITY CENTERS. International Archives of the Photogrammetry, Remote Sensing and Spatial Information Sciences XLII-2/W7, 129–135. https://doi.org/10.5194/isprs-archives-XLII-2-W7-129-2017.

Uchôa, J.G.S.M., Oliveira, P.T.S., Ballarin, A.S., Gastmans, D., Anache, J.A.A., Scanlon, B.R., Camacho, C.R., Freddo Filho, V.J., Wendland, E.C., 2025a. A groundwater well database for Brazil (GWDBrazil). Scientific Data 12, 1582. https://doi.org/10.1038/s41597-025-05843-7.

Uchôa, J.G.S.M., et al., 2025b: A Groundwater Wells Database for Brazil (GWDBrazil) (Version 2). Zenodo [Dataset]. https://doi.org/10.5281/zenodo.16755455.

Wang, B., Shi, W., Miao, Z., 2015. Confidence analysis of standard deviational ellipse and its extension into higher dimensional Euclidean space. PLoS ONE 10, e0118537. https://doi.org/10.1371/journal.pone.0118537.